

# Formation of asteroid pairs by rotational fission

P. Pravec<sup>1</sup>, D. Vokrouhlický<sup>2</sup>, D. Polishook<sup>3</sup>, D. J. Scheeres<sup>4</sup>, A. W. Harris<sup>5</sup>, A. Galád<sup>1,6</sup>, O. Vaduvescu<sup>7,8</sup>, F. Pozo<sup>7</sup>, A. Barr<sup>7</sup>, P. Longa<sup>7</sup>, F. Vachier<sup>9</sup>, F. Colas<sup>9</sup>, D. P. Pray<sup>10</sup>, J. Pollock<sup>11</sup>, D. Reichart<sup>12</sup>, K. Ivarsen<sup>12</sup>, J. Haislip<sup>12</sup>, A. LaCluyze<sup>12</sup>, P. Kušnirák<sup>1</sup>, T. Henych<sup>1</sup>, F. Marchis<sup>13,14</sup>, B. Macomber<sup>13,14</sup>, S. A. Jacobson<sup>15</sup>, Yu. N. Krugly<sup>16</sup>, A. V. Sergeev<sup>16</sup> & A. Leroy<sup>17</sup>

Pairs of asteroids sharing similar heliocentric orbits, but not bound together, were found recently<sup>1–3</sup>. Backward integrations of their orbits indicated that they separated gently with low relative velocities, but did not provide additional insight into their formation mechanism. A previously hypothesized rotational fission process<sup>4</sup> may explain their formation—critical predictions are that the mass ratios are less than about 0.2 and, as the mass ratio approaches this upper limit, the spin period of the larger body becomes long. Here we report photometric observations of a sample of asteroid pairs, revealing that the primaries of pairs with mass ratios much less than 0.2 rotate rapidly, near their critical fission frequency. As the mass ratio approaches 0.2, the primary period grows long. This occurs as the total energy of the system approaches zero, requiring the asteroid pair to extract an increasing fraction of energy from the primary's spin in order to escape. We do not find asteroid pairs with mass ratios larger than 0.2. Rotationally fissioned systems beyond this limit have insufficient energy to disrupt. We conclude that asteroid pairs are formed by the rotational fission of a parent asteroid into a proto-binary system, which subsequently disrupts under its own internal system dynamics soon after formation.

Analyses of the orbits of asteroid pairs reveal some common properties. Asteroid pairs are ubiquitous, being found throughout the main belt and among the Hungaria asteroids<sup>5</sup>. Pair members have low relative velocities, of the order of metres per second in the space of proper elements ( $d_{\text{prop}}$ ): the best studied asteroid pair, 6070–54827, has a relative speed after mutual escape of only  $0.17 \text{ m s}^{-1}$  (ref. 3). They are young, with most pairs having separated less than 1 Myr ago (Supplementary Information). The existence of a population of bound binary systems with a similar range of sizes suggests that related processes may account for both binary formation and pair formation. Previous investigations have indicated that binaries form from parent bodies spinning at a critical rate by some sort of fission or mass shedding process<sup>4,6,7</sup> and that binaries formed by fission will initially have chaotic orbit and spin evolution<sup>8</sup>. The free energy of a binary system formed by fission, defined as the total energy (kinetic and potential) minus the self-potentials of each component<sup>9</sup>, is found here to play a fundamental role in the evolution of a binary. Systems with mass ratios less than  $\sim 0.2$  have a positive free energy and can escape under internal dynamics, whereas systems with greater mass ratios have a negative free energy and cannot so escape. As the system mass ratio approaches this limit, kinetic energy

for escape is drawn from the rotation of the primary (the larger member of the pair), leaving it rotating at a slower rate. This model predicts (1) that primaries of pairs with small mass ratios rotate near to their critical fission period, (2) that as the mass ratio approaches 0.2, the primary period grows long, and (3) that beyond this limit of  $\sim 0.2$ , disruption of the binary is not possible (see Supplementary Information).

We studied the relative sizes, spin rates and shapes of pairs and binaries via a photometric observational program. Our sample consists of 35 asteroid pairs, listed in Table 1. Thirty-two of them were taken from ref. 2, the pair 6070–54827 was from ref. 3, and the pairs 48652–139156 and 229401–2005 UY<sub>97</sub> were identified by backward orbit integrations of the pair's components. The only selection criterion, other than the pair identification procedures used in the above references, was that the pairs occurred in favourable conditions (brightness, position in the sky) for photometric observations with available telescopes. Our sample covers a range of sizes of 1.9–7.0 km for primaries and 1.2–4.5 km for secondaries, with medians of 3.2 km and 1.9 km, respectively, as estimated from the asteroids' absolute magnitudes<sup>6</sup>, assuming geometric albedos according to their orbital group membership<sup>10</sup>.

We integrated orbits of the asteroid pairs backward to 1 Myr before present using techniques developed in refs 1–3, and achieved convergence for 31 of the 35 asteroid pairs in our sample. This strengthened their identification as real, genetically related pairs, and also provided estimates of ages of the pairs ( $T$ ). The four pairs for which convergence was not achieved may be older than 1 Myr (see Supplementary Information).

We estimate the size ratio ( $X$ ) and mass ratio ( $q$ ) between the components of an asteroid pair from the difference between their absolute magnitudes ( $\Delta H \equiv H_2 - H_1$ ), using the relation between an asteroid's absolute magnitude ( $H$ ), effective diameter ( $D$ ) and geometric albedo<sup>6</sup>. Assuming that the components have the same albedo and bulk density, the size ratio is  $X \equiv D_2/D_1 = 10^{-\Delta H/5}$  and the mass ratio is  $q \equiv M_2/M_1 = X^3$ , where  $M_1$  and  $M_2$  are respectively the mass of the primary and the secondary (see Supplementary Discussion 2). A dominating source of uncertainty in the estimates of  $X$  and  $q$  is the uncertainty in the estimated absolute magnitude of each component. For all asteroids in this work, we have used absolute magnitude estimates obtained as a by-product of asteroid astrometric observations published in the AstDyS catalogue (also used in ref. 2). We estimated the mean uncertainty of the catalogue absolute magnitudes

<sup>1</sup>Astronomical Institute AS CR, Fričova 1, CZ-25165 Ondřejov, Czech Republic. <sup>2</sup>Institute of Astronomy, Charles University, V Holešovičkách 2, CZ-18000 Prague, Czech Republic. <sup>3</sup>Wise Observatory and Department of Geophysics and Planetary Sciences, Tel-Aviv University, Tel-Aviv 69978, Israel. <sup>4</sup>Department of Aerospace Engineering Sciences, University of Colorado, Boulder, Colorado 80309, USA. <sup>5</sup>Space Science Institute, 4603 Orange Knoll Avenue, La Canada, California 91011, USA. <sup>6</sup>Modra Observatory, Comenius University, Bratislava SK-84248, Slovakia. <sup>7</sup>Instituto de Astronomía, Universidad Católica del Norte, Avenida Angamos 0610, Antofagasta, Chile. <sup>8</sup>Isaac Newton Group of Telescopes, E-38700 Santa Cruz de la Palma, Canary Islands, Spain. <sup>9</sup>IMCCE-CNRS-Observatoire de Paris, 77 avenue Denfert Rochereau, 75014 Paris, France. <sup>10</sup>Carbuncle Hill Observatory, West Brookfield, Massachusetts 01585, USA. <sup>11</sup>Physics and Astronomy Department, Appalachian State University, Boone, North Carolina 28608, USA. <sup>12</sup>Physics and Astronomy Department, University of North Carolina, Chapel Hill, North Carolina 27514, USA. <sup>13</sup>University of California at Berkeley, Berkeley, California 94720, USA. <sup>14</sup>SETI Institute, Mountain View, California 94043, USA. <sup>15</sup>Department of Astrophysical and Planetary Sciences, University of Colorado, Boulder, Colorado 80309, USA. <sup>16</sup>Institute of Astronomy of Kharkiv National University, Sumska Str. 35, Kharkiv 61022, Ukraine. <sup>17</sup>Observatoire Midi Pyrénées and Association T60, Pic du Midi, France.

**Table 1 | Parameters of asteroid pairs**

Asteroid pair	$d_{\text{prop}}$ (m s <sup>-1</sup> )	$T$ (kyr)	$\Delta H$	$P_1$ (h)	$\delta P_1$ (h)	$U_1$	$A_1$ (mag)	$P_2$ (h)	$\delta P_2$ (h)	$U_2$	$A_2$ (mag)
1979–13732	9.02	>1,000	0.7					8.2987	0.0004	3	0.28
2110–44612	3.36	>1,000	2.2	3.34474	0.00002	3	0.38	4.9070	0.0002	3	0.44
4765–2001 XO <sub>105</sub>	3.49	>90	3.8	3.6260	0.0002	3	0.56				
5026–2005 WW <sub>113</sub>	13.99	17 ± 2	4.1	4.4243	0.0003	3	0.49				
6070–54827	8.09	17.2 ± 0.3	1.5	4.2733	0.0004	3	0.42	5.8764	0.0005	3	0.25
7343–154634	19.91v	>800	2.9	3.7547	0.0004	3	0.20				
9068–2002 OP <sub>28</sub>	34.15v	~32	4.1	3.406	0.004	3	0.20				
10484–44645	0.43	>130	0.9	5.508	0.002	3	0.21				
11842–228747	0.71	>150	2.6	3.68578	0.00009	3	0.13				
15107–2006 AL <sub>54</sub>	2.07	>300	2.6	2.530	0.002	3	0.14				
17198–229056	0.93	>100	2.6	3.2430	0.0002	3	0.13				
19289–2006 YY <sub>40</sub>	6.31v	640 ± 50	2.3	2.85	0.01	3	0.16				
21436–2003 YK <sub>39</sub>	5.88	70 <sup>+70</sup> <sub>-35</sub>	3.3	2.87	0.03	3	0.08				
23998–205383	3.25	>300	1.2	13.526	0.004	3	1.0	5.554	0.004	3	0.30
38707–32957	1.01	>1,000	1.1	6.1509	0.0004		0.36				
40366–78024	27.22v	>350	1.2					>17		2	>0.12
48652–139156	1.38	>650	1.1	13.829	0.004	3	0.63				
51609–1999 TE <sub>221</sub>	1.49	>300	1.5	6.767	0.002	3	0.42				
52773–2001 HU <sub>24</sub>	2.07	>250	2.1	3.7083	0.0003	3	0.35				
52852–2003 SC <sub>7</sub>	1.51	>300	2.0	5.432	0.002	2	0.19				
54041–220143	0.56	>125	1.8	18.86	5	2	0.23	3.502	0.004	3	0.10
56232–115978	40.31v	>60	1.1	5.6	1	2	0.47	2.9	0.4	2	0.11
60744–218099	8.18	350 ± 50	1.1					5.03	0.04	2	0.27
63440–2004 TV <sub>14</sub>	0.21	50 <sup>+55</sup> <sub>-20</sub>	2.3	3.2969	0.0002	3	0.17				
69142–127502	4.81	>400	1.0	7.389	0.002	3	0.55				
76111–2005 JY <sub>103</sub>	0.50	>120	1.8	5.3	0.2	2	0.13				
84203–2000 SS <sub>4</sub>	3.46	>100	1.0	17.73	1	2	0.62				
88259–1999 VA <sub>117</sub>	0.61	60 <sup>+50</sup> <sub>-15</sub>	2.2	4.166	0.002	3	0.12				
88604–60546	1.61	>1,000	1.3	7.178	0.001	3	0.55				
92336–143662	2.82	>300	1.1	28.212	0.002	3	0.44				
101065–2002 PY <sub>103</sub>	1.34	>300	1.8	4.977	0.002	3	0.42				
101703–142694	13.82v	700 ± 100	1.9	3.899	0.001	3	0.29				
139537–210904	6.61	>400	1.5	45	15	2	0.1				
226268–2003 UW <sub>156</sub>	11.23v	>350	1.3	31.2	1.4	2	0.36				
229401–2005 UY <sub>97</sub>	11.57v	17 <sup>+50</sup> <sub>-15</sub>	1.0	28	11	2	0.8				

Data on spin rates of paired asteroids were taken with our photometric observations from the following observatories: Caruncle Hill (West Brookfield, Massachusetts, USA), Cerro Tololo, Dark Sky (University of North Carolina, USA), La Silla, Lick, Maidanak, Modra, Observatoire de Haute-Provence, Pic du Midi and Wise (Tel-Aviv University, Israel). We also include published data for the paired asteroid (9068) 1993 OD (refs 13,14). In total, we estimated rotation periods ( $P$ ) and lightcurve amplitudes ( $A$ ) for 32 primaries (subscript '1') and 8 secondaries (subscript '2') of the 35 asteroid pairs in our sample. (Details given in Supplementary Information.) Suffix 'v' in the second column indicates a long-term instability of the heliocentric orbits that affected (increased) the estimated  $d_{\text{prop}}$  value (ref. 2). The error bars of the  $T$  estimates represent a 90% probability interval estimated as described in Supplementary Information.  $\delta P_1$  and  $\delta P_2$ , standard errors of the estimated periods. In the seventh and eleventh columns, we give quality code ratings ( $U$ ) for the estimated periods, as described in ref. 10.

for our studied paired asteroids to be  $\delta H \approx 0.3$  mag. This propagates to a relative uncertainty in the estimated size ratio of 20%.

Figure 1 presents the observed spin period of the primaries ( $P_1$ ) versus  $\Delta H$  for the 32 primaries studied. These spin rates show a correlation with the mass ratio  $q$  between members of the asteroid pairs. Specifically, primaries of pairs with small secondaries ( $\Delta H > 2.0$ ,  $q < 0.06$ ) rotate rapidly and their spin periods have a narrow distribution from 2.53 h to 4.42 h with a median of 3.41 h, near the critical fission rotation period. As the mass ratio approaches the predicted approximate cut-off limit of 0.2, the primary period grows long. The correlation coefficient between  $\omega_1^2 = (2\pi/P_1)^2$  and  $q$  is  $-0.73$ , and the Student's  $t$  statistic is  $-5.94$  for the number of degrees of freedom of the sample (30), showing that the correlation is significant at a level higher than 99.9% (see Supplementary Information).

It is notable that the distribution of the spin periods of primaries of pairs with small secondaries (see above) is similar to that of the spin periods of primaries of orbiting binaries with similar sizes and size ratios. From a database of binary system parameters<sup>6</sup>, we find that main belt and Hungaria binaries with primary diameters  $D_1 = 2$ –10 km and size ratios  $D_2/D_1 < 0.4$  ( $q < 0.06$ ) have primary rotation periods from 2.21 h to 4.41 h, with a median of 2.92 h.

The observed primary spin rate distribution is consistent with pair formation via the mutual escape of a transient proto-binary system formed from the rotational fission of a critically spinning parent body. In Fig. 1 we show theoretical curves that incorporate constraints on the expected spin period of a primary, assuming a system that is initially fissioned and later undergoes escape. For these computations, systems are given an initial angular momentum consistent with a critical rotation rate, as observed in orbiting binary systems<sup>6</sup>.

Then, assuming conservation of energy and angular momentum, we evaluate the spin period of the larger body if the binary orbit undergoes escape. For simplicity we assume planar systems. Shape ratios of the primary and secondary are incorporated into the energy and angular momentum budget<sup>6</sup> and in conjunction with a range of initial angular momentum values lead to the envelopes shown in Fig. 1. (The mathematical formulation of the model is given in Supplementary Information.)

The observed data for paired asteroids show consistency with the theoretical curves from our simple model described above (a post-fission system of two components starting in close proximity). This starting condition and subsequent process is consistent with the rotational fission model<sup>4,8,11</sup>, which treats the parent asteroid as a contact binary-like asteroid with components resting on each other. A mechanism to spin the asteroid up to its critical rotation frequency is provided by the Yarkovsky–O'Keefe–Radzievskii–Paddack (YORP) effect<sup>12</sup>. When the angular momentum of the system is increased sufficiently, the components can enter orbit about each other: this is what we term rotational fission. The fission spin rate is a function of the mass ratio between the components: for large mass ratios or highly ellipsoidal shapes, the spin period can be significantly longer than the surface disruption limit of a rapidly spinning sphere<sup>4</sup>. The free energy of the proto-binary system is also a strong function of the mass ratio between the components and is relatively independent of the mutual shapes of the pairs that enter fission; the theory<sup>4</sup> predicts that systems with  $q$  less than about 0.20 will have a positive free energy, and that systems with greater mass ratios will have a negative free energy. Taking shapes into account, there is some variability about this value of the mass ratio, which ranges up to 0.28 for more distended shapes<sup>8</sup>.

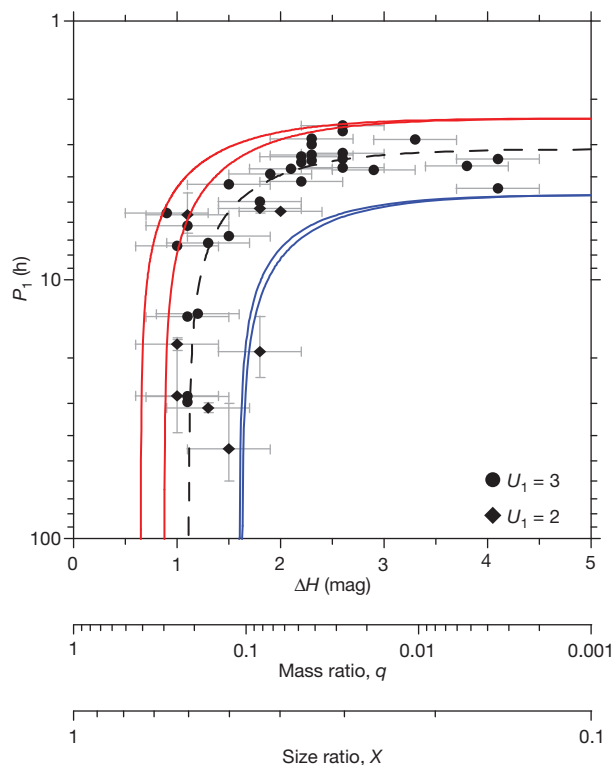


**Figure 1 | Primary rotation periods  $P_1$  versus mass ratios  $q$  of asteroid pairs.** The mass ratio values were estimated from the differences between the absolute magnitudes of the pair components,  $\Delta H$ . The curves were generated with the model of pair separation from the post-fission transient proto-binary. Dashed curve, the set of parameters best representing the properties of the pairs: a system scaled angular momentum  $\alpha_L = 1.0$ , a primary axial ratio  $a_1/b_1 = 1.4$  and an initial orbit's normalized semi-major axis  $A_{\text{ini}}/b_1 = 3$ . Red and blue curves, upper and lower limiting cases, respectively. The upper curves are for  $\alpha_L = 1.2$ ,  $a_1/b_1 = 1.2$ , and  $A_{\text{ini}}/b_1 = 2$  and  $4$ . The lower curves are for  $\alpha_L = 0.7$ ,  $a_1/b_1 = 1.5$ , and  $A_{\text{ini}}/b_1 = 2$  and  $4$ . The choice of  $a_1/b_1 = 1.2$  for the upper limit cases is because the four primaries closest to the upper limit curve have low lightcurve amplitudes  $A_1 = 0.1\text{--}0.2$  mag. Similarly, the choice of  $a_1/b_1 = 1.5$  for the lower limit cases is because the point closest to the lower limit curve has the amplitude  $A_1 = 0.49$  mag, suggesting that the equatorial elongation is  $\sim 1.5$ . Circles, data points with quality code rating  $U_1 = 3$ , meaning a precise period determination; diamonds, data points with  $U_1 = 2$ , which are somewhat less certain estimates (see Table 1 and Supplementary Information). Error bars, standard errors.

Further evidence indicates that asteroid fission as described here may not be the only process at work in the formation of multi-component asteroid systems. There is a disparity between the lightcurve amplitudes of the primary components in asteroid pairs and binary systems (Fig. 2). This cannot be explained by the mechanism of rotational fission alone, as all asteroid systems that undergo rotational fission are initially unstable, regardless of the degree of elongation<sup>8</sup>. Although a more elongated primary may be more efficient at ejecting a secondary, numerical simulations show that ejection can occur even for systems with moderate elongation (Supplementary Information). The above-mentioned disparity in lightcurve amplitudes suggests either that some process occurs during the formation of a stable binary asteroid to give a nearly symmetric primary or that a different formation mechanism is at work<sup>7</sup>. Further observational and theoretical studies must be carried out to discover a cause for this pattern.

The fission mechanism that describes our observations is independent of mineralogical properties, and only depends on mechanical/gravitational interactions between two mass components. This independence, together with the ubiquity of asteroid pairs and binary asteroids, and the occurrence of binaries among the major taxonomic types (S and C), leads us to speculate that the formation of

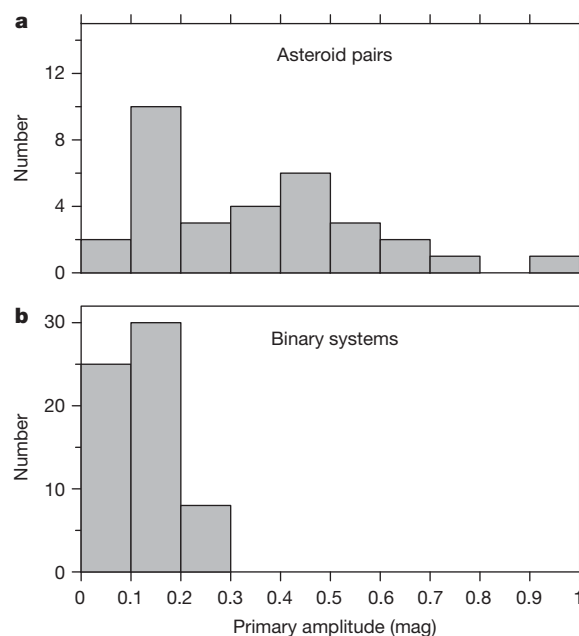


**Figure 2 | A disparity between the lightcurve amplitudes of the primary components in asteroid pairs and binary systems.** The lightcurve amplitudes of primaries of asteroid pairs (a) are distributed relatively randomly, and achieve high values in general, whereas primaries of binary asteroids (b) have more subdued amplitudes. Either asteroids with shapes closer to rotational symmetry are more prone to form stable binaries, or some process occurs during the formation process of a binary asteroid to create such a shape.

asteroid binaries is driven by mechanical and not mineralogical properties.

Received 26 April; accepted 22 June 2010.

- Vokrouhlický, D. & Nesvorný, D. Pairs of asteroids probably of a common origin. *Astron. J.* **136**, 280–290 (2008).
- Pravec, P. & Vokrouhlický, D. Significance analysis of asteroid pairs. *Icarus* **204**, 580–588 (2009).
- Vokrouhlický, D. & Nesvorný, D. The common roots of asteroids (6070) Rheindland and (54827) 2001 NQ8. *Astron. J.* **137**, 111–117 (2009).
- Scheeres, D. J. Rotational fission of contact binary asteroids. *Icarus* **189**, 370–385 (2007).
- Milani, A., Knežević, Z., Novaković, B. & Cellino, A. Dynamics of the Hungaria asteroids. *Icarus* **207**, 769–794 (2010).
- Pravec, P. & Harris, A. W. Binary asteroid population. 1. Angular momentum content. *Icarus* **190**, 250–259 (2007).
- Walsh, K. J., Richardson, D. C. & Michel, P. Rotational breakup as the origin of small binary asteroids. *Nature* **454**, 188–191 (2008).
- Scheeres, D. J. Stability of the planar full 2-body problem. *Celest. Mech. Dyn. Astron.* **104**, 103–128 (2009).
- Scheeres, D. J. Stability in the full two-body problem. *Celest. Mech. Dyn. Astron.* **83**, 155–169 (2002).
- Warner, B. D., Harris, A. W. & Pravec, P. The asteroid lightcurve database. *Icarus* **202**, 134–146 (2009).
- Scheeres, D. J. Minimum energy asteroid reconfigurations and catastrophic disruptions. *Planet. Space Sci.* **57**, 154–164 (2009).
- Botke, W. F. Jr, Vokrouhlický, D., Rubincam, D. P. & Nesvorný, D. The Yarkovsky and Yorp effects: implications for asteroid dynamics. *Annu. Rev. Earth Planet. Sci.* **34**, 157–191 (2006).
- Warner, B. D. Asteroid lightcurve analysis at the Palmer Divide Observatory: 2008 May – September. *Minor Planet Bull.* **36**, 7–13 (2009).
- Galád, A., Kornoš, L. & Világi, J. An ensemble of lightcurves from Modra. *Minor Planet Bull.* **37**, 9–15 (2009).

Supplementary Information is linked to the online version of the paper at [www.nature.com/nature](http://www.nature.com/nature).

**Acknowledgements** Research at Ondřejov was supported by the Grant Agency of the Czech Republic. D.V. was supported by the Czech Ministry of Education. D.P. was supported by an Ilan Ramon grant from the Israeli Ministry of Science, and is grateful for the guidance of N. Brosch and D. Prialnik. D.J.S. and S.A.J. acknowledge support by NASA's PG&G and OPR research programs. A.W.H. was supported by NASA and NSF. Work at Modra Observatory was supported by the Slovak Grant

Agency for Science. The observations at Cerro Tololo were performed with the support of CTIO and J. Vasquez, using telescopes operated by the SMARTS Consortium. Work at Pic du Midi Observatory was supported by CNRS, Programme de Planétologie. Operations at Carbuncle Hill Observatory were supported by the Planetary Society's Gene Shoemaker NEO Grant. Support for PROMPT has been provided by the NSF. F.M. and B.M. were supported by the NSF. We thank O. Bautista, T. Moulinier and P. Eclancher for assistance with observations with the T60 on Pic du Midi.

**Author Contributions** This work was a team effort; here we specify only the most important contributions by individual authors. P.P. led the project and worked on most of its parts, except Supplementary Information sections 1 and 4. D.V. performed the backward orbit integrations and contributed to interpretations of

the results. D.P. ran the observations and data reduction, and contributed to interpretations. D.J.S. developed the fission theory and worked out its implications for the observational data. A.W.H. contributed to interpretations and implications of the data. A.G., O.V., F.P., A.B., P.L., F.V., F.C., D.P.P., J.P., D.R., K.I., J.H., A.L., P.K., T.H., F.M., B.M., Yu.N.K., A.V.S. and A.L. carried out the observations, data reduction and analyses. S.A.J. ran simulations of the satellite ejection process in a proto-binary after fission.

**Author Information** Reprints and permissions information is available at [www.nature.com/reprints](http://www.nature.com/reprints). The authors declare no competing financial interests. Readers are welcome to comment on the online version of this article at [www.nature.com/nature](http://www.nature.com/nature). Correspondence and requests for materials should be addressed to P.P. ([ppravce@asu.cas.cz](mailto:ppravce@asu.cas.cz)).